Soluble Reduced Graphene Oxide Sheets Grafted with Polypyridylruthenium-Derivatized Polystyrene Brushes as Light Harvesting Antenna for Photovoltaic Applications

Zhen Fang,[†] Akitaka Ito,[†,‡] Andrew C. Stuart,[†] Hanlin Luo,[†] Zuofeng Chen,[†] Kizhanipuram Vinodgopal,[§] Wei You,[†] Thomas J. Meyer,[†,*] and Darlene K. Taylor[†,§,*]

[†]Department of Chemistry, Energy Frontier Research Center, University of North Carolina at Chapel Hill, Chapel Hill, North Carolina 27599, United States, [‡]Department of Chemistry, Graduate School of Science, Osaka City University, 3-3-138, Sugimoto, Sumiyoshi-ku, Osaka 558-8585, Japan, and [§]Mary Townes Science Complex, Department of Chemistry, North Carolina Central University, Durham, North Carolina 27707, United States

ABSTRACT Soluble graphene nanosheets, prepared by grafting polystyrene-based polymer chains from the surface of reduced graphene oxide (RGO), have been functionalized with pendant Ru(II) polypyridine chromophores. *N*-Hydroxysuccinimide (NHS) derivatized *p*-vinylbenzoic acid polymer chains were grown from methyl bromoisobutyrate initiation sites on the surface of RGO by atom transfer radical polymerization (ATRP). Deprotection of the resulting NHS polystyrene chains followed by amide coupling with the amine-derivatized Ru(II) polypyridyl complex $[Ru(4\text{-}CH_2NH_2\text{-}4'\text{-}CH_3\text{-}bpy)(bpy)_2]^{2+}$ (4-CH_2NH_2-4′-CH_3-bpy = 4-aminomethyl-4′-methyl 2,2′-bipyridine and bpy = 2,2′-bipyridine) afforded the covalently linked RGO-metallopolymer. The hybrid graphene-polymer assembly has been fully characterized with clear evidence for covalent attachment of the metallopolymer brushes to the graphene substrate. On the basis of thermal gravimetric analysis, one polymer strand is grafted to the surface of RGO for every hundred graphene carbons. The covalently linked polymer brushes feature controlled chain lengths of ∼30 repeat units with a small polydispersity index (PDI, ∼ 1.2). Photovoltaic cells based on the derivatized polymers and graphene-polymer assemblies were evaluated. The graphene-polymer assembly in the configuration, ITO/PEDOT:PSS/RGO-PSRu/$PC_{60}BM$/Al, exhibited enhanced photocurrent and power conversion efficiencies (∼5 fold) relative to devices with the configuration, ITO/PEDOT:PSS/PSRu/$PC_{60}BM$/Al.

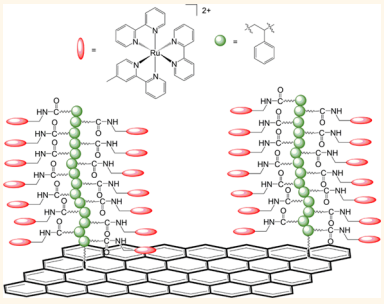

KEYWORDS: graphene · polypyridylruthenium · ATRP · light harvesting

Ruthenium(II) polypyridine complexes have been extensively used as light harvesting chromophores[1−10] and, in combination with polymeric scaffolds, a basis for multichromophoric metallopolymers with potential applications in photosensitization, catalysis and photoenergy conversion.[11−17] One of our interests, tied to the UNC Energy Frontier Research Center on Solar Fuels,[18] is in the development of multichromophoric metallopolymer assemblies anchored to redox-active interfaces for possible use in artificial photosynthesis and solar fuels applications. Initial results on Ru(II) polypyridyl polymers show that these materials offer high optical absorption cross sections, excellent photostability, luminescence, relatively long excited state lifetimes, and efficient electron and energy transport over nanoscale distances. Strategies have evolved for using these materials in photovoltaic applications, so far, with relatively poor conversion efficiencies.[19−21] Closely related ruthenium complexes are used routinely in dye-sensitized solar cells.[22,23] Novel metallopolymer design strategies that incorporate these materials into heterojunctions with efficient electron donor or acceptor

* Address correspondence to tjmeyer@unc.edu, dtaylor@nccu.edu.

Received for review June 18, 2013 and accepted August 17, 2013.

Published online August 17, 2013
10.1021/nn403079z

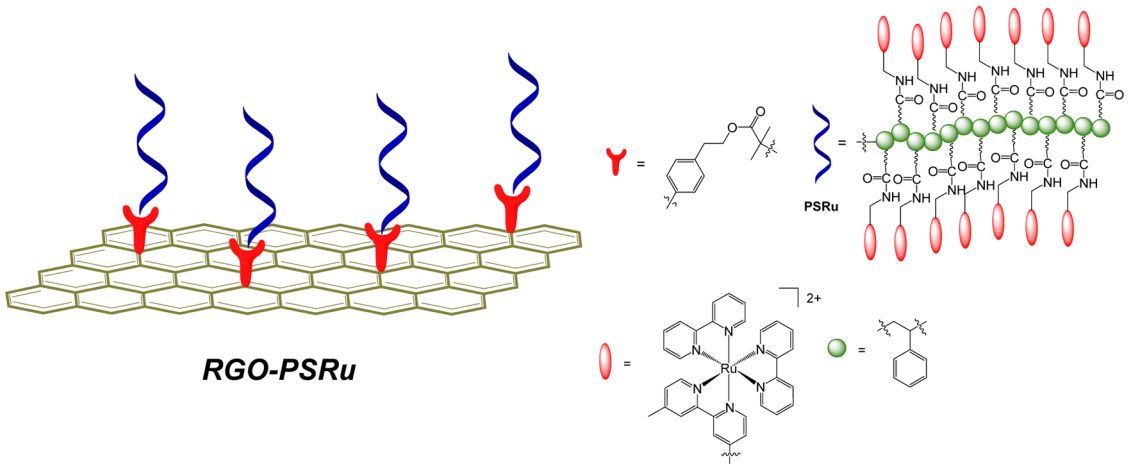

Chart 1. Structure of RGO-PSRu.

materials hold promise in integrating enhanced light absorption/antenna properties with interfacial, photoinduced electron−hole pairs.

Graphene is an exceptional two-dimensional material with excellent structural, chemical, and electrical properties.[24−31] It has opened new strategies for developing a wide range of novel functional materials.[32−35] Redox potentials, mechanical strength, and solubility can all be controlled by functionalization of the graphene surface.[36] Noncovalent modification of graphene sheets with pyrene derivatized ruthenium(II) complexes has been reported, but there have been few reports of Ru(II)-based metallopolymer assemblies covalently linked to graphene. In the pyrene-based approach, the highly conductive sp^2 bond configuration of graphene is preserved, but control and characterization of the inherently unstable supramolecular system limits its usefulness.[37] Ideally, strategies to functionalize graphene should provide enhanced mechanical properties and processability without adversely affecting electrical transport.

A popular chemical modification strategy is to exfoliate graphite to graphene oxide (GO) followed by attachment of polymer chains to the active surface functional groups. There are by now many practical methods to decorate graphene sheets with covalently linked polymers.[38−47] There are, however, no reports of metallopolymer structures covalently grafted to GO such that the polymer brushes are controlled in both density of coverage as well as chain length. Such organized structures are desirable because they can serve as the light harvesting component of assembled organic photovoltaics providing high per unit extinction coefficients that enable full solar spectrum absorption.[48]

In this manuscript, we report on grafting polystyrene (PS) brushes from reduced graphene oxide (RGO) surfaces by atom transfer radical polymerization (ATRP) by using methyl bromoisobutyrate as the initiator. This is the first report, to our knowledge, that takes advantage of the relatively long Ru polypyridyl excited state lifetimes coupled with GO as electron acceptor with a solution processable polymer, chemically grafted onto GO. An additional notable feature is the ability to functionalize the PS polymer brushes with pendant $[Ru(4\text{-}CH_2NH_2\text{-}4'\text{-}CH_3\text{-}bpy)(bpy)_2]^{2+}$ complex units ($4\text{-}CH_2NH_2\text{-}4'\text{-}CH_3$-bpy = 4-aminomethyl-4′-methyl-2,2′- bipyridine and bpy = 2,2-bipyridine) (Chart 1). There appears to be no precedence for preparation of graphene grafted with polypyridyl Ru(II) modified PS brushes with photophysical characterization of the resulting materials.

RESULTS AND DISCUSSION

Synthesis and Characterization. In the linkage chemistry, the methyl bipyridyl ligand of the ruthenium chromophore is attached *via* an amide linkage to the polymer backbone as shown in Scheme 1. The synthetic details of the RGO-PSRu linkage chemistry are reported in the Supporting Information. GO was synthesized by using a modified Hummers procedure.[49,50] The GO was sonicated in the presence of $NaBH_4$ to yield reduced graphene oxide (RGO).[51] The hydroxyl groups of RGO were subsequently modified with 2-bromoisobutyl bromide by a Schötten−Baumann reaction as reported in the literature.[40] ATRP reaction of 2,5-dioxopyrrolidin-1-yl-4-vinylbenzoate (NHVB) was carried out in DMSO at 80 °C with CuBr/1,1,4,7,7-pentamethyldiethylenetriamine (PMDETA) as the catalyst and RGO-methyl bromoisobutyrate as the initiator.

The processes of GO reduction and polymer mobilization were monitored by the ratio of the intensities of the D (~1330 cm^{-1}) and G (~1590 cm^{-1}) bands in the Raman spectra, as shown in Figure 1a. The D band is known to arise from the first order scattering of sp^3 carbons in graphene oxide, while the G band is attributed to the intrinsic sp^2 carbon double bonds. The relative increase intensity of the D band in RGO indicates a decrease of the average size of the sp^2 domains due to the smaller size relative to GO.[51,52]

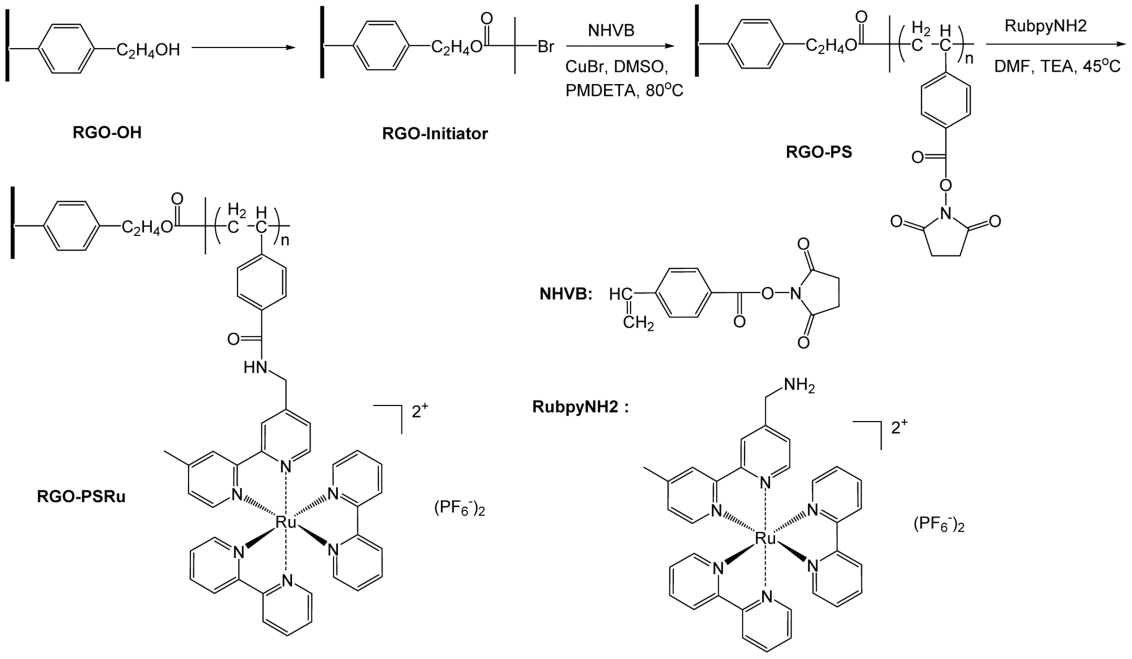

Scheme 1. Synthesis of RGO-PSRu.

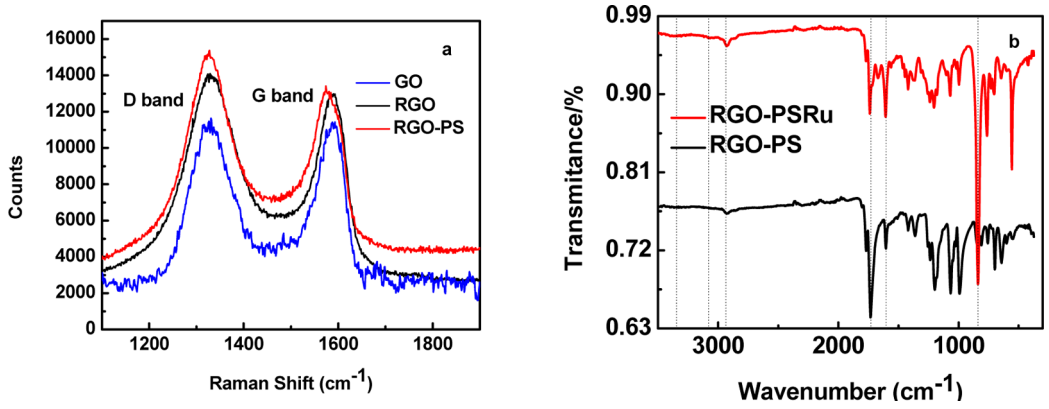

Figure 1. Raman spectra of GO, RGO and hybrid (a), and ATR-IR spectra of RGO-PSRu and RGO-PS films (b).

When polymer was grafted *in situ* to RGO, a slight increase in the D band and a shift of G bands indicate the formation of chemical bonds between RGO and polymer chains.[46]

The length of the polymer chain on graphene was determined by gel permeation chromatography (GPC) with DMF as the eluent. In order to characterize the PS brush, it was detached from the graphene surface by treatment with NaOH. ^{1}H NMR showed that the functional side groups on the polystyrene backbone were hydrolyzed to yield the parent carboxylic acid functional groups. On the basis of the GPC results, the unattached polymer is estimated to be ~30 repeat units long.

The extent of hydroxyl functionalization can be estimated by thermal gravimetric analysis (TGA) under N_2. As shown in Figure S1 (Supporting Information), a comparison of GO, RGO, RGO-OH, and RGO-initiator shows a weight loss at 120 °C corresponding to residual −COOH groups with GO undergoing two continuous decompositions at 400 °C presumably due to the hydroxyl and epoxy groups. On the basis of this assumption, the mass loss observed at 340 °C is attributed to the decomposition of the C−O−C link nearest to graphene. A 15% weight loss for RGO-OH at 340 °C corresponds to 17.5 hydroxyl groups per 1000 graphene carbons, which is similar to the literature value.[40] However, we only observe a 21% loss in RGO-initiator at 340 °C, corresponding to 10 initiators per 1000 graphene carbons. On the basis of this observation, we estimate that the average ratio of polymer brushes to graphene carbons in the RGO-PSRu hybrid is 1:100. Considering that the polymer chain has 30 repeat units (as determined from GPC measurements on the detached polymer), a RGO-PSRu solution at a concentration of 5 μM in Ru contains ~0.2 mg/L of graphene. At half loading (i.e., only ~50% of the side chains on the polymer backbone end-capped with Ru(II) chromophore), there is 0.4 mg/L of graphene.

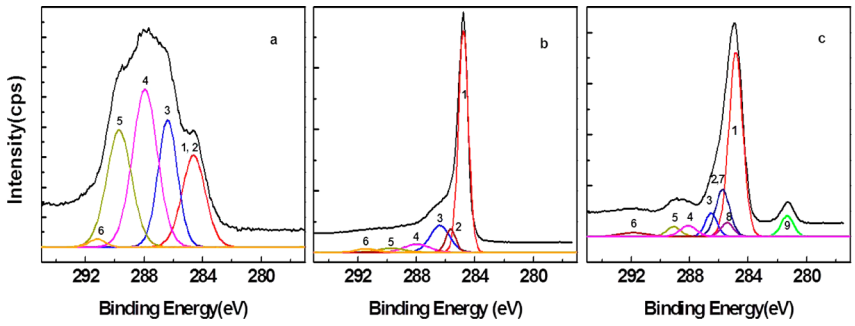

Figure 2. The C 1s peak in the XPS spectra and fitting curves for GO (a), RGO (b), and RGO-PSRu (c). The curves were fit to C═C (sp^2, peak 1); C—C (sp^3, peak 2); C—O/C—O—C (hydroxyl and epoxy groups, peak 3); C═O (carbonyl, peak 4); O—C═O (carboxyl, peak 5); and $\pi-\pi^*$ (peak 6); C—N (amide, 7); Ru 3d (8, 9).

RGO-PS was functionalized by stirring a DMF suspension of the $RubpyNH_2$ derivatized complex catalyzed by triethylamine. A continuous Soxhlet extraction removed the excessive $RubpyNH_2$ to levels undetectable by UV—vis measurements. The proton NMR spectrum of the hybrid in DMSO-d_6 is identical to the spectrum of free PSRu. Previous results obtained on conjugated poly(3-hexylthiophene) revealed a small chemical shift for downfield protons when the polymer was attached to the surface of graphene.[53] However, the average repeat unit of the Ru complex on the polymer chain is at a relatively long distance from the graphene, core and the resulting weak electronic interactions apparently do not lead to a significant effect on chemical shifts.

Steric hindrance and static electronic repulsion prevented complete substitution of the PS side groups with Ru(II)(polypyridyl) units. The infrared spectrum of RGO-PSRu films include a broad band arising from residual —COOH residues at ~3300 cm^{-1} providing evidence for incomplete transamidation and subsequent hydrolysis (Figure 1b). However, the decreased intensity for the carbonyl stretching mode at 1730 cm^{-1} and increase at 1630 cm^{-1} suggest that a considerable fraction of the PS side groups have been substituted with the Ru complex. The band at 1630 cm^{-1} arises from the carbonyl stretching mode of the imide in RGO-PS transformed to an amide group in RGO-PSRu. The sharp band at ~834 cm^{-1} arises from an asymmetric stretch in the PF_6^- counterion and the band at 3080 cm^{-1} from the N—H stretching mode of the secondary amide group in RGO-PSRu.

Although the pendant groups are not fully loaded with Ru units, previous studies using electron acceptors like 9,10-anthraquinone-2,6-disulfonate (AQS) report fast energy migration between the Ru units in the polymer with quenching observed by intrastrand electron transfer from the nearest excited Ru site to the AQS.[54] The earlier results point to a possible related mechanism for excited state quenching in RGO-PSRu. In this case excitation followed by energy transfer migration to the site or sites nearest the graphene surface provides a mechanism for electron transfer quenching. Electron transfer quenching is favored with the excited state Ru^{III}/Ru^{II*} potential at $E_{ox}^* = -3.8$ V *versus* the free electron in a vacuum compared to the work function for graphene oxide at −4.42 eV.[55] Further details are presented in the photophysical and electrochemistry sections.

X-ray Photoelectron Spectroscopy (XPS). Figure 2 shows C 1s XPS and corresponding fitted spectra for GO, RGO, and RGO-PSRu. As shown in Figure 2a, the C 1s peak for GO consists of four major components of comparable intensities. They appear at 284.6, 286.4, 287.9, and 289.7 eV arising from ionizations of the C═C/C—C, C—O/C—O—C (hydroxyl and epoxyl), C═O (carbonyl), and O—C═O (carboxyl), bonds, respectively. A relatively weak $\pi-\pi^*$ component at ~291.9 eV is also observed. Although the C 1s XPS spectrum of RGO exhibits the same functionalities as GO with identical binding energies, the intensities of the carbonyl and carboxyl groups are substantially reduced (Figure 2b), as are intensities for C—O bond ionizations. These results are consistent with reports in the literature and suggest almost complete reduction of GO.[51]

Figure 2c shows ionization energies arising from the Ru 3d electrons at 281.3 (Peak 9) and 285.4 eV (Peak 8), corresponding to $3d^{5/2}$ and $3d^{3/2}$, respectively. The intensity of the ~286.5 eV feature increases because of an overlap of intensities arising from the C—N and C—C ionizations. These observations coupled with our RGO-PSRu purification procedures, detailed in Supporting Information, enable us to conclude with confidence that the polypyridylruthenium complex derivatized polymer brushes have been successfully grafted onto the surface of RGOs.

Photophysical Properties. Photograph images of GO, RGO, PSRu and RGO-PSRu in DMF solutions are shown in Figure S2 (Supporting Information). Figure 3a shows the normalized absorption spectra of the PSRu polymer and of RGO-PSRu in DMF solutions. Both show absorption bands characteristic of the Ru(II) polypyridyl complexes. The intense absorption band centered at ~460 nm arises from a metal-to-ligand charge transfer (MLCT), $Ru^{II} \rightarrow$ bpy, absorption. It is slightly red-shifted and broadened when grafted onto graphene in RGO-PSRu.

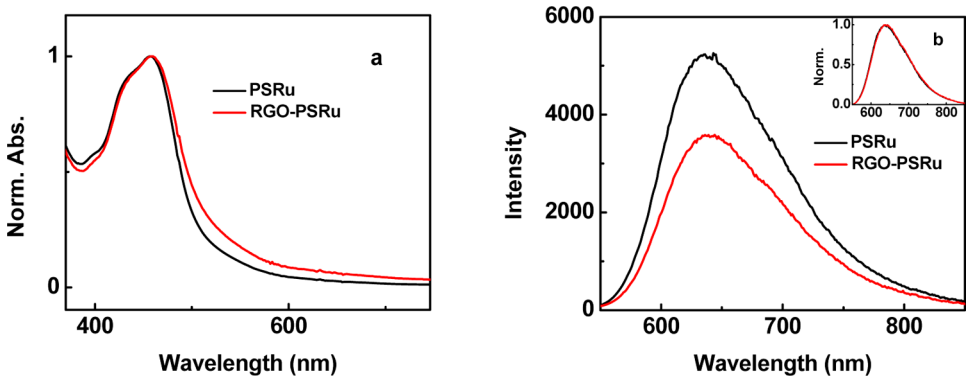

Figure 3. Absorption (a) and emission (b) spectra of PSRu and RGO-PSRu in DMF, [Ru] = 5 μM. Relative emission intensities are reflective of relative quantum yields. Inset in (b) is the normalized emission spectra of PSRu and RGO-PSRu. Excitation at 460 nm.

The red-shift may arise from overlapping absorption with RGO given its long absorption tail in the UV−vis and IR range (see Figure S3, Supporting Information) or to light scattering. Electronic interactions between Ru complex chromophores and RGO seem unlikely to be the origin of the shifts given the NMR evidence for noninteracting sites.

The steady-state emission spectra of PSRu and RGO-PSRu in Figure 3b in DMF were obtained in deoxygenated DMF solutions excited at 460 nm at room temperature. Both feature a broad and moderately intense emission maximized at ~640 nm arising from MLCT Ru^{II}* excited state emission. The fact that the emission spectra for $RubpyNH_2$, PSRu and RGO-PSRu are essentially identical (see Figure S4, Supporting Information), with only differences in relative emission quantum yields, is consistent with noninteracting metal complex chromophore units in the polymer brushes without substantial aggregation or strong interchromophore interaction. Notable is the partial quenching effect of introducing RGO into the hybrid with RGO capable of acting as an energy/charge trapping site for the MLCT excited state.

To illustrate the impact of graphene on the Ru-MLCT excited state, control experiments were conducted with RGO/PSRu bimolecular quenching (see Figure S5, Supporting Information). The concentrations of RGO ranged from 0 to 1.25 mg/L with the latter comparable to the ratio of graphene to polymer in RGO-PSRu hybrid. Upon the addition of RGO to the PSRu solution, only slight emission quenching was observed. The Stern−Volmer constant (K_{SV}) is calculated to be ~10^3 L^{-1} g^{-1}.

Emission decay profiles were monitored at 630 nm to illustrate the quenching mechanism (Figure S5, Supporting Information). The Stern−Volmer plot of lifetime decay (τ_0/τ) is similar to the quantum yield decay (Φ_0/Φ), indicating that the quenching of PSRu emission by RGO is dominated by diffusional electron transfer between PSRu and RGO. Compared to the emission quenching of the physical mixture system, the amplified quenching of the emission observed in the RGO-PSRu hybrid in Figure 3b provides confirmation that the polymer backbone with the pendant Ru chromophore is indeed chemically bound to the RGO surface. It is also notable that the excitation spectrum (monitored at the emission maximum at 640 nm) for RGO-PSRu is identical to that for PSRu (see Figure S6, Supporting Information), in agreement with the absorption and emission spectra. There is no evidence in the excitation spectrum for aggregation of RGO-PSRu in solution.

The results of the absorption and emission spectra are consistent with the ability of RGO to act as an electron acceptor resulting in emission quenching of the MLCT excited state in isolated RGO-PSRu hybrids. The extent of quenching in the hybrid is comparable to that observed in a closely related PSRu polymer with an electron transfer acceptor end group where long-range site-to-site energy transfer migration followed by electron transfer quenching at the end group was proposed.[53,58]

Electrochemistry. A saturated solution of RGO-PSRu in DMF was drop-cast on the surface of indium doped tin oxide (ITO) on glass and dried in a vacuum overnight for cyclic voltammetry (CV) measurements. For comparison purposes, two control samples were prepared on ITO glass electrodes, one with free polymer PSRu and the other coated with a blended sample of PSRu with RGO. Figure 4 shows cyclic voltammograms of all three samples. All of them display reversible oxidation waves with $E_{1/2}(Ru^{III/II})$ = 0.95 V *versus* Fc^+/Fc (1.50 V *versus* NHE). This potential is comparable to $E_{1/2}(Ru^{III/II})$ for $Ru(bpy)_3(PF_6)_2$ under the same conditions.

The CVs of PSRu and the blended sample of PSRu and RGO include reversible redox waves at $E_{1/2}$ = −1.66, −1.91, −2.19 V *versus* Fc^+/Fc arising from sequential reduction of the three bipyridine ligands on the Ru complex. These potentials are comparable to values for $Ru(bpy)_3(PF_6)_2$ consistent with an absence of significant interactions between the ligands at adjacent Ru sites on the derivatized polymer. Also,

comparison of the CVs from PSRu and the RGO/PSRu blend reveal no evidence for significant interaction between PSRu and RGO in the blend. However, PSRu is covalently attached to graphene in RGO-PSRu; the ligand-based redox processes become quasi-reversible with currents for the reoxidation of ligands greatly diminished; note that the black reduction wave in Figure 4 and $E_{1/2}$ for the first ligand reduction is shifted ~70 mV more positively in RGO-PSRu compared to PSRu. The observation may arise from RGO stabilization of the ligand radical anion with the resulting electronic interactions opening an electronic channel for RGO to shuttle electrons as observed in graphene and carbon nanotube hybrids.[53,56]

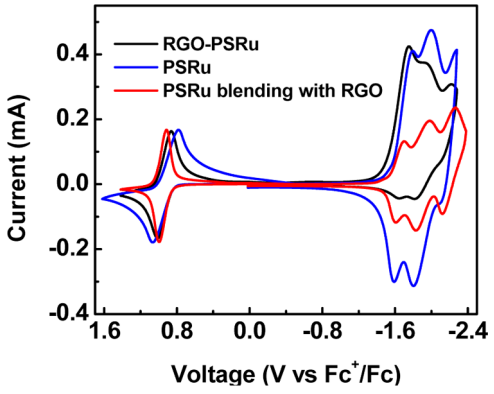

Figure 4. CVs of PSRu, RGO-PSRu and a blend of RGO with PSRu on ITOs: 0.1 M Bu_4NPF_6 in deoxygenated CH_3CN, with a Pt wire as the counter electrode, a $Ag/AgNO_3$ as reference *versus* ferrocence/ferrocenium at −0.19 V, scan rate = 100 mV s^{-1}.

Morphological Properties. The cationic pendant Ru units enable dissolution of RGO-PSRu in DMF yielding a transparent solution, which remains stable for several months (Figure S2, Supporting Information). Atomic force microscopy (AFM) images of exfoliated GO and RGO-PSRu hybrid on mica substrates, obtained by spin-coating and drying in a vacuum, are shown in Figure 5. The nanosheets of GO and RGO-PSRu show irregular shapes with sizes ranging from tens of nanometers to several micrometers. The height profiles show that the thickness of the GO sheets is ~1.1 nm, which is in agreement with GO thicknesses reported in the literature (~0.8−1.5 nm).[15] Figure 5b shows bright spots on noncontinuous membranes formed by RGO-PSRu suggesting aggregates. The measured height of RGO-PSRu in this case increased to ~10 nm (Figure 5b). The thickness of RGO-initiator has been reported to be ~2.2−3 nm, where the substituted aryl groups on both sides of GO contribute ~0.6 × 2 nm.[39,57] A PSRu polymer with 10 repeat units has a chain length of ~30 Å. Thus, compared to GO, the 9 nm increase in thickness can be attributed to the surface-attached polymers.

Similar observations have been made in scanning electron microscopy (SEM) and transmission electron microscopy (TEM) images (Figure S7 and S8, respectively, Supporting Information). Thin flakes of GO were distributed on substrates with sizes ranging from several nanometers to ~1 μm, consistent with the AFM results. Single layers of transparent GO flakes apparently have been converted to smaller RGO pieces accompanied with some multiple layer sheets.

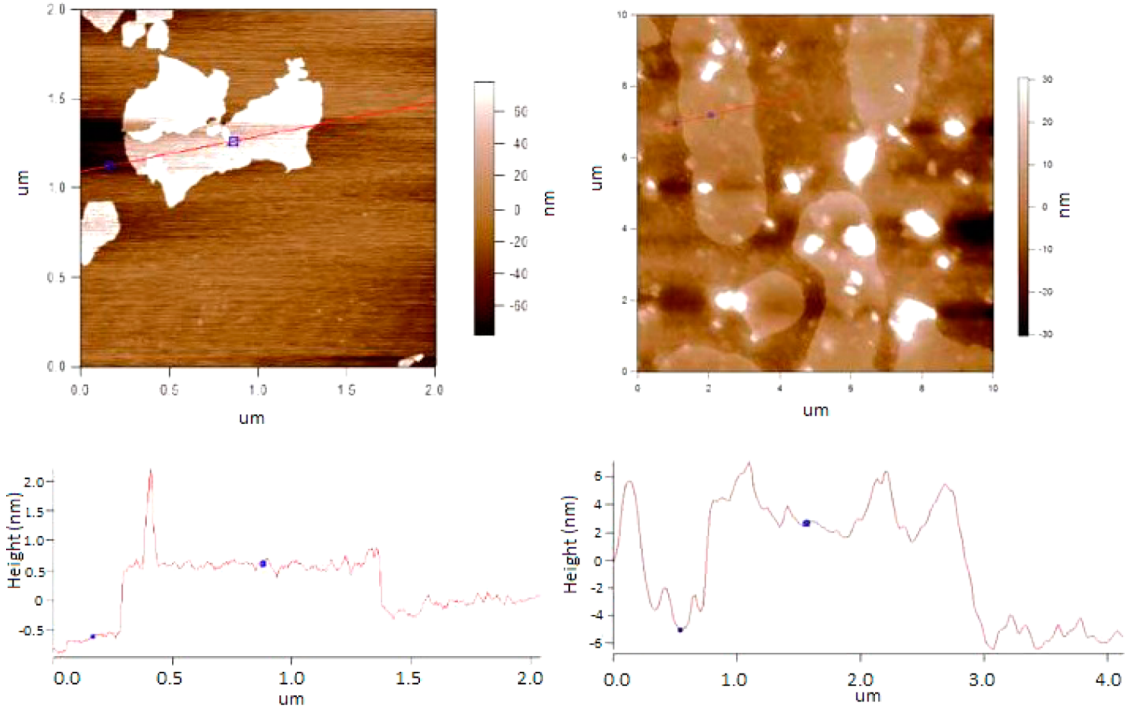

Figure 5. AFM images of GO (a) and RGO-PSRu (b) together with the height profiles from a cross-section analysis.

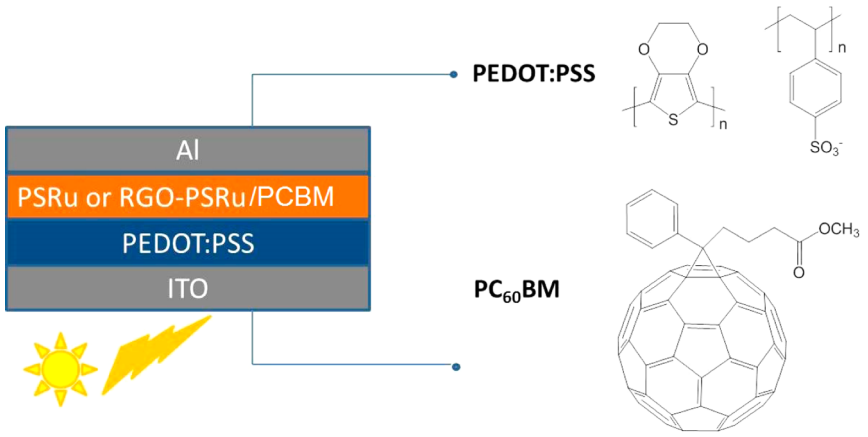

Figure 6. Device configuration and structures of PEDOT:PSS and $PC_{60}BM$.

Poor solubility of RGO in water and DMF has been explained as being due to reduced amounts of hydroxyl/carboxyl groups, which accounts for the aggregates in the SEM image of RGO. Once functionalized with the polypyridyl ruthenium oligomer, the RGO adduct was converted into a noncontinuous membrane with agglomerate formation as shown in Figure S7c (Supporting Information). In spite of the abundance of agglomerate in the hybrid, one can observe the RGO sheets covered with a smooth surface of polymer in the hybrid TEM image.

Photovoltaic Characterization. Photovoltaic cells, configured as ITO/PEDOT:PSS/PSRu (RGO-PSRu)/$PC_{60}BM$/Al, were fabricated as shown in Figure 6 with details presented in the Supporting Information. The anode was indium-doped tin oxide (ITO). The structure of PEDOT:PSS, poly(3,4-ethylenedioxythiophene):poly(styrenesulfonate), is shown in Figure 6. The origin of the photovoltaic effect for the RGO-PSRu hybrid arises following MLCT excitation of the polymer-bound Ru(II)-polypyridyl chromophores. For this chromophore, visible excitation is dominated by transitions to low lying metal-to-ligand charge transfer (MLCT) excited states largely single in character followed by rapid (psec) conversion to the lowest triplet with the net process, $Ru^{II}(bpy)^{2+} \xrightarrow{h\nu} {}^3[Ru^{III}(bpy^-)^{2+*}]$. This state is capable of transferring electrons to either PCBM and/or RGO as acceptor.

The excited state redox potential for the couple $Ru^{III}(bpy)^{3+} + e^- \rightarrow {}^3[Ru^{III}(bpy^-)^{2+*}]$ on PSRu (E_{ox}*) can be calculated from the free energy content of the excited state above the ground state, ΔG_{ES}, which is available from Franck–Condon fitting of the emission spectral profiles and eq 1.[58,59]

$$\Delta G_{ES} = E_0 + \frac{(\Delta \upsilon_{1/2})^2}{16 k_B T \ln 2} \quad (1)$$

In eq 1, E_0 is the $v = 0 \rightarrow v^* = 0$ energy gap, $\Delta \upsilon_{1/2}$ is the vibronic bandwidth at half-height, and k_B and T are the Boltzmann constant and absolute temperature, respectively. A complicating feature, observed earlier,

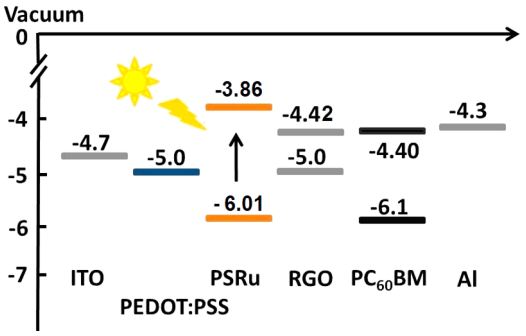

Figure 7. Energy diagram of ITO/PEDOT:PSS/PSRu/RGO/$PC_{60}BM$/Al.

and attributable to rapid intrastrand energy transfer migration in the PSRu polymers, is the appearance of a time dependence in emission spectra.[60,61] Following excitation, energy migration occurs to low energy "trap" sites on the polymers, which, because of the small energy gaps, dominate excited state decay. Application of the single-mode Franck–Condon analysis to time dependent emission spectra for PSRu at long times when equilibration had occurred gave E_0 = 1.98 eV (~16 000 cm^{-1}, see Figure S9 and fitting parameters in Table S1, Supporting Information). The values of $\Delta \upsilon_{1/2}$, k_B, and T are 1700 cm^{-1}, 0.70 cm^{-1} K^{-1}, and 298 K, respectively. On the basis of these values, ΔG_{ES} = 2.14 eV, $E_{ox}^* = E_{ox} - \Delta G_{ES}/nF = -0.64$ V *versus* NHE, 3.86 eV *versus* vacuum with F, the Faraday, in eV per equivalent.

An energy diagram for the ITO/PEDOT:PSS/PSRu/RGO/$PC_{60}BM$/Al configuration is shown in Figure 7. A photocurrent density versus voltage plot is presented in Figure 8. In the energy diagram, a common ΔG_{ES} value is assumed for polymer chromophores in PSRu and RGO-PSRu. From the PV measurements, the devices have similar open circuit potentials (V_{oc}) with V_{oc} = 0.1 V as expected given the common E_{ox}* values. The theoretical V_{oc} is the difference between the excited state redox potential on the polymer and the $PC_{60}BM$ LUMO energy.

In the absence of graphene, $^3[Ru^{III}(bpy^-)^{2+}*]$ excited states migrate along individual polymer strands by intrastrand energy transfer hopping among the pendant Ru sites and finally to a PCBM junction where oxidative quenching occurs by electron transfer from $^3[Ru^{III}(bpy^-)^{2+}*]$ to PCBM. Once formed, the $Ru^{III}(bpy)^{3+}$ sites are transported back along the polymer chain to a Ru/PEDOT interface where oxidation of PEDOT regenerates $Ru^{II}(bpy)^{2+}$. An energy/electron transfer hopping mechanism is illustrated in Figure 9.

The presence of RGO in the graphene hybrid structure provides an additional electron/energy transfer pathway for utilization of the $^3[Ru^{III}(bpy^-)^{2+}*]$ excited states. The graphene work function has been estimated to be −4.4 eV *versus* vacuum.[62] With RGO, energy transfer migration of $^3[Ru^{III}(bpy^-)^{2+}*]$ along the polymer strands to the RGO interface results in oxidative quenching, $^3[Ru^{III}(bpy^-)^{2+}*]$ RGO → $Ru^{III}(bpy)^{3+}$ RGO^-, followed by RGO^- electron transfer to the $PC_{60}BM$ acceptor. Because of depletion of sp^3 character in reduced graphene oxide, a significantly decreased charge-transfer resistance in the RGO/$PC_{60}BM$ film is expected. This creates an electron transfer conduction network facilitating electron transfer to $PC_{60}BM$, accounting for the considerable photocurrent enhancement for RGO-PSRu (0.11 mA·cm^{-2}) compared to PSRu (0.02 mA·cm^{-2}).

Nonetheless, photocurrents and power conversion efficiencies are low with a maximum of ∼0.003% for the latter, in large part due to limited light absorption. The limited solubility of PSRu and RGO-PSRu in dichlorobenzene resulted in very thin active layers for light harvesting. In addition, aggregation in the RGO-PSRu films may also play a role by inhibiting charge separation and collection at the interfaces between polymer and PCBM and polymer and PEDOT:PSS. Aggregation was observed in AFM images (Figure 5). From the energy diagram, the $^3[Ru^{III}(bpy^-)^{2+}*]$ excited state is sufficiently oxidized to undergo electron transfer to the LUMO of PCBM. However, E_{ox} levels are closer to the HOMO of PCBM, which suggests possible hole transfer at the interface between polymer and PCBM with extensive electron−hole recombination at the interface.

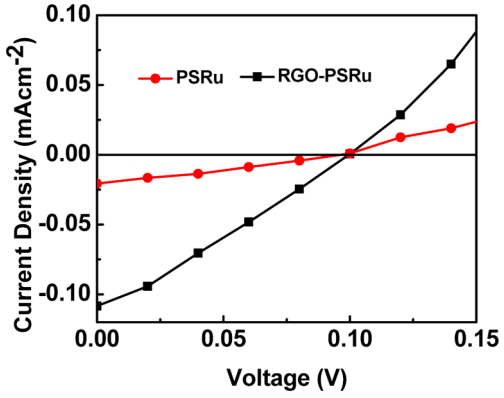

Figure 8. Current density−voltage curves of ITO/PEDOT:PSS/PSRu (RGO-PSRu)/$PC_{60}BM$/Al.

In a prior study on Ru(II)-bpy containing polymers with conjugated polymer frameworks, higher photocurrents (∼1−2 mA·cm^{-2})[19,20] were observed than for our nonconjugated polystyrene backbones. Higher ground state potentials in the conjugated polymer lower the hole injection barrier from oxidized chromophore to PEDOT:PSS and may inhibit electron−hole recombination at the polymer/PCBM interface, a reaction that occurs in the inverted region.[21]

CONCLUSIONS

In summary, surface initiated ATRP enables the preparation of a soluble graphene that is grafted with polypyridylruthenium derivatized polystyrene. The appearance of this chemically linked hybrid demonstrates an accessible strategy for grafting even charged transition metal complexes to the surface of graphene. The product, obtained as RGO-PSRu in DMF solution, has been fully characterized. We estimate that 1 out of every 100 graphene carbons contains a polymer chain (PSRu) in RGO-PSRu by thermal gravimetric analysis. Photophysical experiments confirm that PSRu is chemically bonded to graphene in RGO-PSRu, resulting in quenched emission. Cyclic voltammetry measurements also reflect an interaction between GO and the PSRu units. Because of the unique electronic properties of graphene, GO, and the Ru complex polymers, these are novel hybrids with considerable potential for light harvesting applications in optoelectronic devices.

Photovoltaic cells ITO/PEDOT:PSS/PSRu (RGO-PSRu)/$PC_{60}BM$/Al were fabricated and characterized. Because of the graphene aggregation and electron−hole recombination, the power conversion efficiencies are

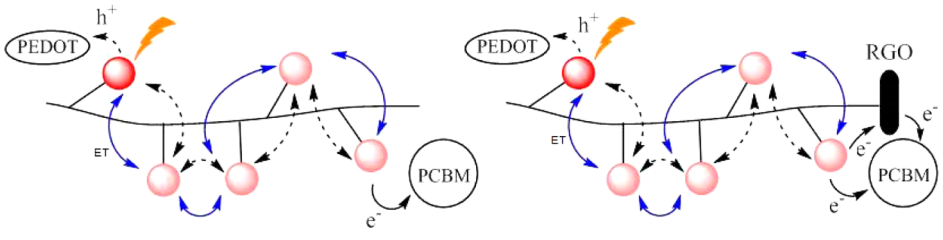

Figure 9. Proposed energy/charge transfer mechanisms.

low. However, in comparison with the device made from PSRu, the one with RGO-PSRu exhibits enhanced photocurrent and conversion efficiency (over 5 fold), which shows the advantages of the graphene/metallopolymer hybrid. A focus for future work could be on minimizing graphene aggregation and tuning the energy levels for better photovoltaic performance.

MATERIALS AND METHODS

NMR spectra were obtained in $CDCl_3$ and/or DMSO-d_6 on a Bruker instrument operating at 300 MHz. Gel permeation chromatography (GPC) analyses were conducted on a Waters Alliance System comprised of a Waters 2695 Separations Module and Waters 2414 Refractive Index Detector (Waters Associates Inc., Milford, MA). A polystyrene standard kit was used for molecular weight elution volume calibration. IR spectra were collected on a Bruker ALPHA FT-IR spectrometer equipped with an attenuated total reflection (ATR) sampling accessory. UV–vis absorption spectra were recorded on a Hewlett-Packard 8453 spectrometer. Steady-state emission spectra were recorded on an Edinburgh Instruments FLS920 emission spectrometer, equipped with a Xenon light source. Emission intensities at each wavelength were corrected for system spectral response. Cyclic voltammetry was carried out on a computer-controlled CHI660D electrochemical workstation, where a ITO glass served as the working electrode, a platinum electrode as the counter electrode, and a 0.1 M $AgNO_3$/Ag electrode as the reference. A solution of tetrabutylammonium hexafluorophosphate (0.1 M) in dry acetonitrile was used as the supporting electrolyte, and the scan rate was 100 mV s^{-1}.

Synthesis. Graphene oxide (GO) was synthesized using a modified Hummers procedure, followed by reduction with $NaBH_4$ in the presence of sonication to yield RGO.[51] The RGO-initiator was synthesized according to the literature.[40] All reagents were used as received unless otherwise specified. 1,1,4,7,7-Pentamethyldiethylenetriamine (PMDETA) was purchased from Sigma-Aldrich and used without further purification. $RubpyNH_2$ was synthesized on the basis of previous report.[60] Copper(I) bromide was sequentially treated with acetic acid, ethanol, and acetone before use. 2,5-Dioxopyrrolidin-1-yl-4-vinylbenzoate (NHVB) was synthesized according to the literature.[63] Free polymer PSRu was prepared elsewhere.[60] All reactions were carried out under nitrogen or argon flow unless otherwise noted.

Photovoltaic Cells Fabrication and Characterization. ITO conducting glasses (25Ω/sq) were sonicated in acetone and isopropanol for 15 min each and treated in O_2 plasma for 15 min. A PEDOT:PSS film was prepared from the aqueous solution by spin coating, followed by annealing at 180 °C for 20 min. A solution containing PSRu or RGO-PSRu:$PC_{60}BM$ (1:4 by weight) in *o*-dichlorobenzene:DMF (1:1) was spin coated on PEDOT:PSS/ITO glass and then annealed at 110 °C for 45 min. A thin film (100 nm) of Al was thermally evaporated on the top of active layer under a vacuum of 10^{-6} Torr. All devices were then annealed in air at 110 °C for 15 min.

Conflict of Interest: The authors declare no competing financial interest.

Acknowledgment. Support from the UNC EFRC: Center for Solar Fuels, an Energy Frontier Research Center funded by the U.S. Department of Energy, Office of Science, Office of Basic Energy Sciences under Award Number DE-SC0001011 supporting Z.F., A.S., and Z.C. is acknowledged. A.I. acknowledges support from the U.S. Department of Energy, Office of Science, Office of Basic Energy Sciences, under Award Number DE-FG02-06ER15788. We thank the Chapel Hill Analysis and Nanofabrication Laboratory, Institute for Advanced Materials, University of North Carolina, for XPS, AFM, and SEM microscopy measurements.

Supporting Information Available: Additional synthesis details, thermal gravity analysis (TGA), absorption and emission spectra of control experiments, and excitation spectra of RGO-PSRu, SEM and TEM images, Franck–Condon emission spectral fitting and the parameters. This material is available free of charge *via* the Internet at http://pubs.acs.org.

REFERENCES AND NOTES

1. Kent, C. A.; Mehl, B. P.; Ma, L.; Papanikolas, J. M.; Meyer, T. J.; Lin, W. Energy Transfer Dynamics in Metal-Organic Frameworks. *J. Am. Chem. Soc.* **2010**, *132*, 12767–12769.
2. Concepcion, J. J.; House, R. L.; Papanikolas, J. M.; Meyer, T. J. Chemical Approaches to Artificial Photosynthesis. *Proc. Natl. Acad. Sci. U. S. A.* **2012**, *109*, 15560–15564.
3. Fang, Y. Q.; Taylor, N. J.; Laverdiere, F.; Hanan, G. S.; Loiseau, F.; Nastasi, F.; Campagna, S.; Nierengarten, H.; Leize-Wagner, E.; Van Dorsselaer, A. Ruthenium(II) Complexes with Improved Photophysical Properties Based on Planar 4′-(2-Pyrimidinyl)-2,2′:6′,2″-terpyridine Ligands. *Inorg. Chem.* **2007**, *46*, 2854–2863.
4. Cooke, M. W.; Hanan, G. S.; Loiseau, F.; Campagna, S.; Watanabe, M.; Tanaka, Y. Self-Assembled Light-Harvesting Systems: Ru(II) Complexes Assembled about Rh-Rh Cores. *J. Am. Chem. Soc.* **2007**, *129*, 10479–10488.
5. Loiseau, F.; Nastasi, F.; Stadler, A. M.; Campagna, S.; Lehn, J. M. Molecular Wire Type Behavior of Polycationic Multinuclear Rack-Type RuII Complexes of Polytopic Hydrazone-Based Ligands. *Angew. Chem., Int. Ed. Engl.* **2007**, *46*, 6144–6147.
6. Medlycott, E. A.; Hanan, G. S.; Loiseau, F.; Campagna, S. Tuning the Excited-State Energy of the Organic Chromophore in Bichromophoric Systems Based on the Ru(II) Complexes of Tridentate Ligands. *Chem.—Eur. J.* **2007**, *13*, 2837–2846.
7. Tuccitto, N.; Torrisi, V.; Cavazzini, M.; Morotti, T.; Puntoriero, F.; Quici, S.; Campagna, S.; Licciardello, A. Stepwise Formation of Ruthenium(II) Complexes by Direct Reaction on Organized Assemblies of Thiol-Terpyridine Species on Gold. *ChemPhysChem* **2007**, *8*, 227–230.
8. Borisov, S. M.; Wolfbeis, O. S. Optical Biosensors. *Chem. Rev.* **2008**, *108*, 423–461.
9. Sassolas, A.; Leca-Bouvier, B. D.; Blum, L. J. DNA Biosensors and Microarrays. *Chem. Rev.* **2008**, *108*, 109–139.
10. Szacilowski, K.; Macyk, W.; Drzewiecka-Matuszek, A.; Brindell, M.; Stochel, G. Bioinorganic Photochemistry: Frontiers and Mechanisms. *Chem. Rev.* **2005**, *105*, 2647–2694.
11. Hjelm, J.; Constable, E. C.; Figgemeier, E.; Hagfeldt, A.; Handel, R.; Housecroft, C. E.; Mukhtar, E.; Schofield, E. A Rod-like Polymer Containing (Ru(terpy)2) Units Prepared by Electrochemical Coupling of Pendant Thienyl Moieties. *Chem. Commun. (Cambridge, U. K.)* **2002**, 284–285.
12. Liu, Y.; Jiang, S.; Schanze, K. S. Amplified Quenching in Metal-Organic Conjugated Polymers. *Chem. Commun. (Cambridge, U. K.)* **2003**, 650–651.
13. Serin, J. M.; Brousmiche, D. W.; Frechet, J. M. Cascade Energy Transfer in a Conformationally Mobile Multichromophoric Dendrimer. *Chem. Commun. (Cambridge, U. K.)* **2002**, 2605–2607.
14. Walters, K. A.; Trouillet, L.; Guillerez, S.; Schanze, K. S. Photophysics and Electron Transfer in Poly(3-octylthiophene) Alternating with Ru(II)- and Os(II)-Bipyridine Complexes. *Inorg. Chem.* **2000**, *39*, 5496–5509.
15. Dreyer, D. R.; Park, S.; Bielawski, C. W.; Ruoff, R. S. The Chemistry of Graphene Oxide. *Chem. Soc. Rev.* **2010**, *39*, 228–240.
16. Fleming, C. N.; Brennaman, M. K.; Papanikolas, J. M.; Meyer, T. J. Efficient, Long-Range Energy Migration in Ru(II) Polypyridyl Derivatized Polystyrenes in Rigid Media. Antennae for Artificial Photosynthesis. *Dalton Trans.* **2009**, 3903–3910.
17. Fleming, C. N.; Maxwell, K. A.; DeSimone, J. M.; Meyer, T. J.; Papanikolas, J. M. Ultrafast Excited-State Energy Migration

Dynamics in an Efficient Light-Harvesting Antenna Polymer Based on Ru(II) and Os(II) Polypyridyl Complexes. *J. Am. Chem. Soc.* **2001**, *123*, 10336–10347.
18. Meyer, T.; Papanikolas, J.; Heyer, C. Solar Fuels and Next Generation Photovoltaics: The UNC-CH Energy Frontier Research Center. *Catal. Lett.* **2011**, *141*, 1–7.
19. Duprez, V.; Biancardo, M.; Spanggaard, H.; Krebs, F. C. Synthesis of Conjugated Polymers Containing Terpyridine-Ruthenium Complexes: Photovoltaic Applications. *Macromolecules* **2005**, *38*, 10436–10448.
20. Cheung, W. K.; Mak, C. S. K.; Chan, W. K. Heteroleptic Ruthenium (II) Complex-Containing Polymers and Their Bandgap Tuning and Photosensitizing Properties. *Macromol. Rapid Commun.* **2012**, *33*, 585–591.
21. Man, K. Y. K.; Wong, H. L.; Chan, W. K. Use of a Ruthenium-Containing Conjugated Polymers as a Photosensitizer in Photovoltaic Devices Fabricated by a Layer-by-Layer Deposition Process. *Langmuir* **2006**, *22*, 3368–3375.
22. Grätzel, M. Solar Energy Conversion by Dye-Sensitized Photovoltaic Cells. *Inorg. Chem.* **2005**, *44*, 6841–6851.
23. Chiba, Y.; Islam, A.; Watanabe, Y.; Komiya, R.; Koide, N.; Han, L. Dye-Sensitized Solar Cells with Conversion Efficiency of 11.1%. *Jpn. J. Appl. Phys., Part 2* **2006**, *45*, L638–L640.
24. Fasolino, A.; Los, J. H.; Katsnelson, M. I. Intrinsic Ripples in Graphene. *Nat. Mater.* **2007**, *6*, 858–861.
25. Balandin, A. A.; Ghosh, S.; Bao, W.; Calizo, I.; Teweldebrhan, D.; Miao, F.; Lau, C. N. Superior Thermal Conductivity of Single-Layer Graphene. *Nano Lett.* **2008**, *8*, 902–907.
26. Guo, S.; Dong, S. Graphene Nanosheets: Synthesis, Molecular Engineering, Thin Film, Hybrids, and Energy and Analytical Applications. *Chem. Soc. Rev.* **2011**, *40*, 2644–2672.
27. Bunch, J. S.; Verbridge, S. S.; Alden, J. S.; Van der Zande, A. M.; Parpia, J. M.; Craighead, H. G.; McEuen, P. L. Impermeable Atomic Membrances from Graphene Sheets. *Nano Lett.* **2008**, *8*, 2458–2462.
28. Du, X.; Skachko, I.; Barker, A.; Andrei, E. Y. Approaching Ballistic Transport in Suspended Graphene. *Nat. Nanotechnol.* **2008**, *3*, 491–495.
29. Becerril, H. A.; Mao, J.; Liu, Z.; Stoltenberg, R. M.; Bao, Z.; Chen, Y. Evaluation of Solution-Processed Reduced Graphene Oxide Films as Transparent Conductors. *ACS Nano* **2008**, *2*, 463–470.
30. Lee, C.; Wei, X.; Kysar, J. W.; Hone, J. Measurement of the Elastic Properties and Intrinsic Strength of Monolayer Graphene. *Science* **2008**, *321*, 385–388.
31. Tombros, N.; Jozsa, C.; Popiniuc, M.; Jonkman, H. T.; van Wees, B. J. Electronic Spin Transport and Spin Precession in Single Graphene Layers at Room Temperature. *Nature* **2007**, *448*, 571–574.
32. Jo, K.; Lee, T.; Choi, H. J.; Park, J. H.; Lee, D. J.; Lee, D. W.; Kim, B. S. Stable Aqueous Dispersion of Reduced Graphene Nanosheets *via* Non-Covalent Functionalization with Conducting Polymers and Application in Transparent Electrodes. *Langmuir* **2011**, *27*, 2014–2018.
33. Li, X.; Wang, X.; Zhang, L.; Lee, S.; Dai, H. Chemically Derived, Ultrasmooth Graphene Nanoribbon Semiconductors. *Science* **2008**, *319*, 1229–1232.
34. Villar-Rodil, S.; Paredes, J. I.; Martinez-Alonso, A.; Tascon, J. M. D. Preparation of Graphene Dispersions and Graphene-Polymer Composites in Organic Media. *J. Mater. Chem.* **2009**, *19*, 3591–3593.
35. Robinson, J. T.; Perkins, F. K.; Snow, E. S.; Wei, Z.; Sheehan, P. E. Reduced Graphene Oxide Molecular Sensors. *Nano Lett.* **2008**, *8*, 3137–3140.
36. Yan, X.; Li, B.; Cui, X.; Wei, Q.; Tajima, K.; Li, L.-S. Independent Tuning of the Band Gap and Redox Potential of Graphene Quantum Dots. *J. Phys. Chem. Lett.* **2011**, *2*, 1119–1124.
37. Li, S.; Zhong, X.; Yang, H.; Hu, Y.; Zhang, F.; Niu, Z.; Hu, W.; Dong, Z.; Jin, J.; Li, R.; et al. Noncovalent Modified Graphene Sheets with Ruthenium(II) Complexes Used as Electrochemiluminescent Materials and Photosensors. *Carbon* **2011**, *49*, 4239–4245.
38. Steenackers, M.; Gigler, A. M.; Zhang, N.; Deubel, F.; Seifert, M.; Hess, L. H.; Lim, C. H. Y. X.; Loh, K. P.; Garrido, J. A.; Jordan, R.; et al. Polymer Brushes on Graphene. *J. Am. Chem. Soc.* **2011**, *133*, 10490–10498.
39. Fang, M.; Wang, K.; Lu, H.; Yang, Y.; Nutt, S. Single-Layer Graphene Nanosheets with Controlled Grafting of Polymer Chains. *J. Mater. Chem.* **2010**, *20*, 1982–1992.
40. Wang, D.; Ye, G.; Wang, X. Graphene Functionalized with Azo Polymer Brushes: Surface-Initiated Polymerization and Photoresponsive Properties. *Adv. Mater.* **2011**, *23*, 1122–1125.
41. Fowler, J. D.; Allen, M. J.; Tung, V. C.; Yang, Y.; Kaner, R. B.; Weiller, B. H. Practical Chemical Sensors from Chemically Derived Graphene. *ACS Nano* **2009**, *3*, 301–306.
42. Yang, Y.; Wang, J.; Zhang, J.; Liu, J.; Yang, X.; Zhao, H. Exfoliated Graphite Oxide Decorated by PDMAEMA Chains and Polymer Particles. *Langmuir* **2009**, *25*, 11808–11814.
43. Lee, S. H.; Dreyer, D. R.; An, J.; Velamakanni, A.; Piner, R. D.; Park, S.; Zhu, Y.; Kim, S. O.; Bielawski, C. W.; Ruoff, R. S. Polymer Brushes *via* Controlled, Surface-Initiated Atom Transfer Radical Polymerization (ATRP) from Graphene Oxide. *Macromol. Rapid Commun.* **2010**, *31*, 281–288.
44. Goncalves, G.; Marques, P. A. A. P.; Barros-Timmons, A.; Bdkin, I.; Singh, M. K.; Emami, N.; Gracio, J. Graphene Oxide Modified with PMMA *via* ATRP as a Reinforcement Filler. *J. Mater. Chem.* **2010**, *20*, 9927–9934.
45. Sun, S.; Cao, Y.; Feng, J.; Wu, P. Click Chemistry as a Route for the Immobilization of Well-Defined Polystyrene onto Graphene Sheets. *J. Mater. Chem.* **2010**, *20*, 5605–5607.
46. Fang, M.; Wang, K.; Lu, H.; Yang, Y.; Nutt, S. Covalent Polymer Functionalization of Graphene Nanosheets and Mechanical Properties of Composites. *J. Mater. Chem.* **2009**, *19*, 7098–7105.
47. Qi, X.; Pu, K.-Y.; Zhou, X.; Li, H.; Liu, B.; Boey, F.; Huang, W.; Zhang, H. Conjugated-Polyelectrolyte-Functionalized Reduced Graphene Oxide with Excellent Solubility and Stability in Polar Solvents. *Small* **2010**, *6*, 663–669.
48. Islam, A.; Chowdhury, F. A.; Chiba, Y.; Komiya, R.; Fuke, N.; Ikeda, N.; Nozaki, K.; Han, L. Synthesis and Characterization of New Efficient Tricarboxyterpyridyl (β-diketonato) Ruthenium(II) Sensitizers and Their Applications in Dye-Sensitized Solar Cells. *Chem. Mater.* **2006**, *18*, 5178–5185.
49. Hummers, W. S.; Offeman, R. E. Preparation of Graphitic Oxide. *J. Am. Chem. Soc.* **1958**, *80*, 1339–1339.
50. Xu, Y.; Bai, H.; Lu, G.; Li, C.; Shi, G. Flexible Graphene Films *via* the Filtration of Water-Soluble Noncovalent Functionalized Graphene Sheets. *J. Am. Chem. Soc.* **2008**, *130*, 5856–5857.
51. Shin, H.-J.; Kim, K. K.; Benayad, A.; Yoon, S.-M.; Park, H. K.; Jung, I.-S.; Jin, M. H.; Jeong, H.-K.; Kim, J. M.; Choi, J.-Y.; et al. Efficient Reduction of Graphite Oxide by Sodium Borohydride and Its Effect on Electrical Conductance. *Adv. Funct. Mater.* **2009**, *19*, 1987–1992.
52. Stankovich, S.; Dikin, D. A.; Piner, R. D.; Kohlaas, K. A.; Kleinhammes, A.; Jia, Y.; Wu, Y.; Nguyen, S. T.; Ruoff, R. S. Synthesis of Graphene-Based Nanosheets *via* Chemical Reduction of Exfoliated Graphite Oxide. *Carbon* **2007**, *45*, 1558–1565.
53. Yu, D.; Yang, Y.; Durstock, M.; Baek, J.-B.; Dai, L. Soluble P3HT-Grafted Graphene for Efficient Bilayer−Heterojunction Photovoltaic Devices. *ACS Nano* **2010**, *4*, 5633–5640.
54. Sun, Y.; Chen, Z.; Puodziukynaite, E.; Jenkins, D. M.; Reynolds, J. R.; Schanze, K. S. Light Harvesting Arrays of Polypyridine Ruthenium(II) Chromophores Prepared by Reversible Addition−Fragmentation Chain Transfer Polymerization. *Macromolecules* **2012**, *45*, 2632–2642.
55. Wang, X.; Zhi, L.; Mullen, K. Transparent, Conductive Graphene Electrodes for Dye-Sensitized Solar Cells. *Nano Lett.* **2008**, *8*, 323–327.
56. Bavastrello, V.; Carrara, S.; Ram, M. K.; Nicolini, C. Optical and Electrochemical Properies of Poly(o-toluidine) Multiwalled Carbon Nanotubes Composite Langmuir-Schaefer Films. *Langmuir* **2004**, *20*, 969–973.
57. Lomeda, J. R.; Doyle, C. D.; Kosynkin, D. V.; Hwang, W.-F.; Tour, J. M. Diazonium Functionalization of Surfactant-Wrapped Chemically Converted Graphene Sheets. *J. Am. Chem. Soc.* **2008**, *130*, 16201–16206.

58. Ito, A.; Meyer, T. J. The Golden Rule. Application for Fun and Profit in Electron Transfer, Energy Transfer, and Excited-State Decay. *Phys. Chem. Chem. Phys.* **2012**, *14*, 13731–13745.
59. Ito, A.; Stewart, D. J.; Knight, T. E.; Fang, Z.; Brennaman, K.; Meyer, T. J. Excited-State Dynamics in Rigid Media: Evidence for Long-Range Energy Transfer. *J. Phys. Chem. B* **2013**, *117*, 3428–3438.
60. Fang, Z.; Ito, A.; Keinan, S.; Chen, Z.; Watson, Z.; Rochette, J.; Kanai, Y.; Taylor, D.; Schanze, K.; Meyer, T. Atom Transfer Radical Polymerization Preparation and Photophysical Properties of Polypyridylruthenium Derivatized Polystyrenes. *Inorg. Chem.* **2013**, *52*, 8511–8520.
61. Dupray, L. M.; Devenney, M.; Striplin, D. R.; Meyer, T. J. An Antenna Polymer for Visible Energy Transfer. *J. Am. Chem. Soc.* **1997**, *119*, 10243–10244.
62. Tang, Y.-B.; Lee, C.-S.; Xu, J.; Liu, Z.-T.; Chen, Z.-H.; He, Z.; Cao, Y.-L.; Yuan, G.; Song, H.; Chen, L.; et al. Incorporation of Graphenes in Nanostructured TiO_2 Films *via* Molecular Grafting for Dye-Sensitized Solar Cell Application. *ACS Nano* **2010**, *4*, 3482–3488.
63. Aamer, K. A.; Tew, G. N. RAFT Polymerization of a Novel Activated Ester Monomer and Conversion to a Terpyridine-Containing Homopolymer. *J. Polym. Sci., Part A: Polym. Chem.* **2007**, *45*, 5618–5625.